A Simple Method for Forecast of Cooling Time of High-Density Polyethylene During Gas-Assisted Injection Molding

Shui-Po Liang,[1] Bin Yang,[1] Xiao-Rong Fu,[2] Wei Yang,[1] Nan Sun,[1] Sheng Hu,[1] Ming-Bo Yang[1]

[1]*College of Polymer Science and Engineering, State Key Laboratory of Polymer Materials Engineering, Sichuan University, Chengdu 610065, People's Republic of China*
[2]*College of Chemical Engineering, Sichuan University, Chengdu 610065, People's Republic of China*

Received 21 March 2009; accepted 10 August 2009
DOI 10.1002/app.31259
Published online 24 March 2010 in Wiley InterScience (www.interscience.wiley.com).

ABSTRACT: Gas-assisted injection molding (GAIM) is an innovative plastic processing technology, which was developed from the conventional injection molding, and has currently found wide industrial applications. About 70% of the whole gas-assisted injection molding cycle is actually occupied by the cooling stage. The quality and production efficiency of molded parts are considerably affected by the cooling stage. Hence, it is necessary to study the solidification behaviors during the cooling stage. In this work, a simple experimental method was designed to simulate the solidification behaviors of high-density polyethylene during cooling stage of GAIM. The enthalpy transformation approach, coupled with the control-volume/finite difference techniques, was adopted to deal with the transient heat transfer problems with phase change effects. *In situ* measurements of the temperature decreases in the cavity were also carried out. Reasonable agreements between the experimental values and the simulated results such as cooling time, cooling rates, and temperature curves were obtained, which proved that this simple experimental method was effective. © 2010 Wiley Periodicals, Inc. J Appl Polym Sci 117: 729–735, 2010

Key words: simulation; gas-assisted injection molding; temperature field; polyethylene; enthalpy

INTRODUCTION

As is known, gas-assisted injection molding (GAIM), which was developed from the conventional injection molding (CIM), has become one of the significant polymer processing techniques, especially for the manufacturing of hollow articles since 1990s.[1] GAIM has drawn great attention in recent years because it can reduce clamping tonnage, cycle time, and save raw materials, etc. In comparison with CIM, the problems such as warpage, sink marks, and stress concentration can be relatively well settled.[2,3] GAIM cycle usually consists of three steps and can be described as follows: the mold cavity is partially filled with the polymer melts, and after a period of delay time, compressed gas subsequently penetrates into the molten polymer and drives it into the mold end. Then, the solidification process will continue till a demolding temperature is reached, and the time for which the solidification process takes is known as cooling time, as illustrated in Figure 1.

During the GAIM process, there is a complex dynamic interactions among the melt, gas and solid phase, such as the hard and soft constrained boundary conditions (the flexible gas/melt interface and the rigid melt/wall interface), as well as the complex multiple flow process (the melt filling flow, the local melt flow associated with the gas penetration, etc). Therefore, the GAIM process is more complex as compared with CIM. Up to now, studies regarding GAIM can be classified into three groups: first, the numerical simulations of the gas penetration and residual wall thickness;[4–6] second, the optimal designs of GAIM process as well as the product design of the GAIM parts;[7–9] third, the morphologies and structures in the GAIM parts of PE, PP, PC, PA, as well as their composites and blends.[10–12] Thus, the understanding of the morphology evolutions during GAIM may supply a better insight into the interrelation between processing and structures under real processing conditions.

Correspondence to: M.-B. Yang (yangmb@scu.edu.cn) or X.-R. Fu (xrfu666@scu.edu.cn).

Contract grant sponsor: National Natural Science Foundation of China; contract grant numbers: 50673067, 20734005.
Contract grant sponsor: Major State Basic Research Projects; contract grant number: 2005CB623808.
Contract grant sponsor: National College Student Innovative Research Projects of Sichuan University; contract grant number: 011.

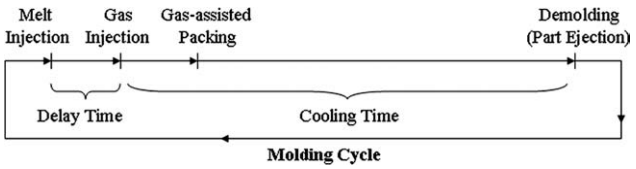

Figure 1 Schematic representation of a typical GAIM cycle.

Moreover, the morphologies (e.g., shish-kebab, oriented lamellae, and banded spherulites) observed in the GAIM parts are significantly affected by a number of factors involved during the cooling stage of the GAIM process.[13–15] Besides, some defects (such as the sink marks and air bubble) are also related with the cooling stage of the GAIM process. As a result, study on the solidification behaviors and the cooling time during GAIM process is of significance to both industrial applications and further investigations of crystalline structures.

So far, many methods have been developed to solve the transient heat conduction problems, such as solidification/melting,[16] the variational method,[17,18] the moving heat source method,[19,20] the perturbation method,[21,22] as well as the numerical methods.[23–25] Among these methods, the numerical methods have been widely used in the solution of multidimensional phase change heat transfer issues. The enthalpy transformation methodology proposed by Cao and Faghri[26] was a commonly used numerical method, which had been proved to be applicable for the generalized multidimensional phase change issues with phase-change zone. In our previous work, based on experimental and theoretical studies of the temperature distribution during the cooling stage in GAIM and CIM processes, it is evident that the enthalpy transformation method could effectively forecast the cooling rates.[27–30]

Generally, under the experimental conditions because of the lack of *in situ* instrument, predicting the cooling time of the GAIM process is not accurate and direct. Thus, to find a simple and effective method for the prediction of the cooling stage of the GAIM process may be significant for the future work on the crystal morphologies of the GAIM parts and the optimization of the parameters during the GAIM process.

EXPERIMENTAL PART

Materials and sample preparation

The material used in this work was a commercial-grade high-density polyethylene (HDPE), (Model 2911), obtained from Fushun Petrochemical, P.R. China, with a weight-average molecular weight (M_w) of 1.4×10^5 g/mol and a melt flow rate of 20.0 g/10 min (190°C/2.16 kg, ASTMD1238). For the calculation, the thermal parameters and the solid and liquid densities of high-density polyetheylene were provided with detailed descriptions elsewhere.[30] Figure 2 shows the sample prepared in this study. To ensure the accuracy of the experiment, 10 pieces of the samples were prepared.

DSC Characterizations

The measurements were carried out on a differential scanning calorimeter (DSC), (TA-Q 20) in a nitrogen atmosphere to test the nonisothermal crystallization process. The sample was initially heated to 215.0°C and maintained for 4.0 min to remove the thermal history. Subsequently, the sample was cooled to the ambient temperature. Then, the latent heat H and phase change temperature range T_1–T_2 were obtained as 109.5–123.1°C.

Experimental instruments and procedures

Figure 3 shows the instrument used in this study. To experimentally validate the calculated results, a specially-designed device was applied, i.e., a metallic container (with a certain amount of HDPE at the bottom) together with a micro-thermocouple (measuring range: 35–350°C, average standard error range: ±1.0 to 1.5%, sensor tip diameter: 0.5 mm). The micro-thermocouple was fixed on the container and inserted into the resins (at the bottom of the container), and the inserting depth could be just half of the thickness of the molten polymer. The whole device was initially

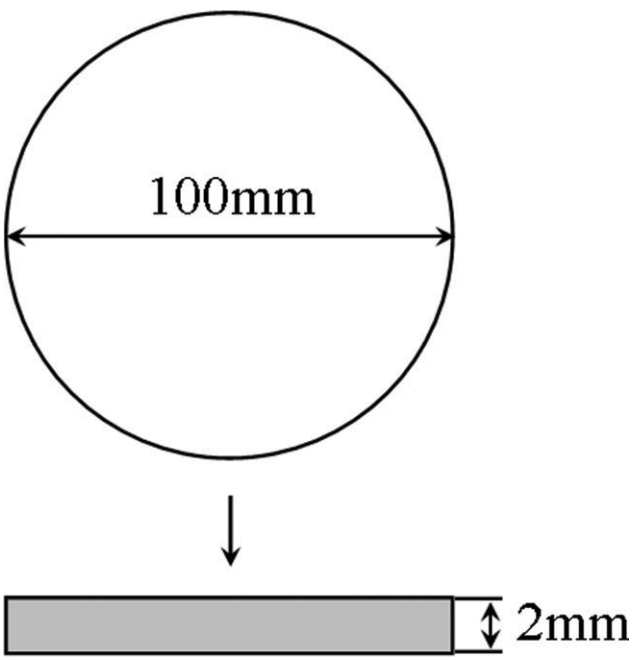

Figure 2 Schematic of the dimensions of the sample prepared for the *in situ* temperature measurements.

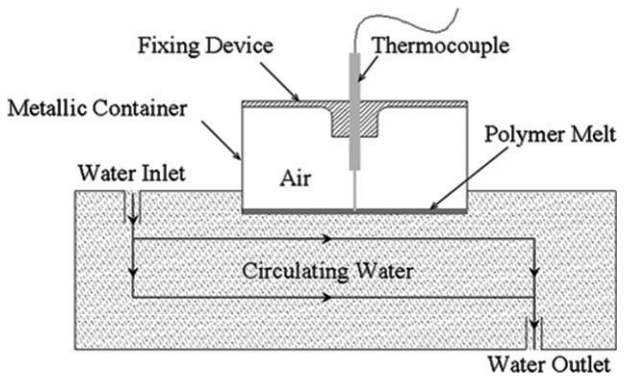

Figure 3 Schematic of the experimental instrument for the *in situ* temperature measurements.

heated to 190.0°C and kept for 4.0 min at this temperature. Subsequently, the metallic container was quickly put into a reservoir filled with water at the ambient temperature (15.0°C). For better simulating the cooling stage of the GAIM process, the water was circulated via the inlet and outlet as the cooling water in the mold, which shown in Figure 3. The temperature decreases during the whole cooling stage were recorded by the Keithley Data Acquisition System (with sampling time: 0.05 s).

MATHEMATICAL MODELING

The cooling model and assumptions

Figure 4 shows the basic principles of the present cooling model. As the container was put into the reservoir, the polymer melt in direct contact with the container wall solidified immediately. A solid/liquid phase interface was formed once the container wall contacted the cold water (see Fig. 4). As the time elapses, the heat was transferred through the gas/melt interface and container wall/melt interface (as shown in Fig. 4). As the thermal diffusivity of the metallic container wall and water are much greater than the gas, the solid/liquid phase interface was moving toward the gas/melt interface, and when two interfaces met, the whole cooling stage was over. As the length and the width of the solidify polymer are 10 times more than the thickness, this solidification process can be treated as a one-dimensional heat transfer problem.

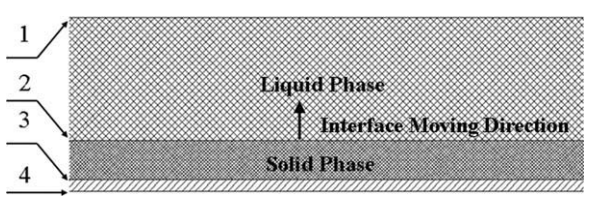

Figure 4 Basic principle of the cooling model: 1. gas/melt interface; 2. solid/liquid phase interface; 3. container wall/melt interface; and 4. container wall/ water interface.

In the present simulations, combined with our previous work and assumptions,[27–29] the main assumptions used are as follows: first of all, the initial condition, an initial temperature T_0, which is higher than the polymer phase-change temperature range T_1–T_2, is adopted. As far as the boundary conditions are concerned, on the gas/melt boundary, the gas temperature is T_g, a convective boundary condition is assigned. On the water side, because of the large thermal diffusivity of the water and the metallic container wall, thermal conduction mechanism with phase changes should be used. No thermal resistances were assumed between the metallic container wall and the water, as well as between the metallic container wall and the polymer melt. The skin polymer near the container wall has the same temperature T_w with the water. Therefore, the container wall has the temperature T_w, which is the temperature of water and is lower than the polymer phase change temperature range. The initial and boundary conditions of the cooling model are shown in Figure 5.

On the other hand, we assume that the solidification process begins immediately as the container was put into the cold water. The incompressibility of the melt (no density changes) is also assumed, so the thermal convection between the liquid and solid phase can be negligible. At the same time, the thermal parameters of the polymer such as the thermal conductivity and specific heat capacity are assumed to be constant.

In this numerical calculation, the heat conduction can be assumed to be within the thickness direction as that in our previous simulations in GAIM process,[30,31] because the ratio of width and thickness (W/L) is $\leq$10 in this case. In addition, as a matter of fact, owing to the polydispersity and hierarchical structures, polymer melts actually solidify over a temperature range, rather than at a single temperature. Therefore, the phase transformation of crystalline polymer is assumed to take place over a temperature range T_1–T_2, and $T_m = (T_1 + T_2)/2$ was used as a reference temperature in this case, which is approximately the crystallization temperature of the polymer.[30] The latent heat will be simultaneously released during the phase-change process.

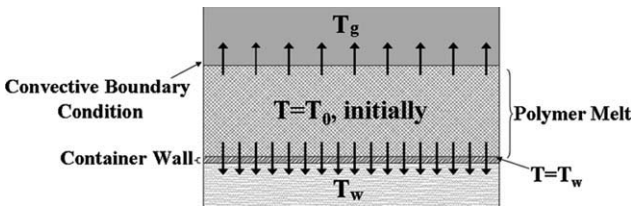

Figure 5 Schematic of the initial and boundary conditions in the cooling model.

Enthalpy transformation and finite-difference treatment

The energy equation coupled the continuity equation in the Cartesian coordinate system is,[32]

$$\rho \cdot C_p \cdot \frac{DT}{Dt} = \nabla(k \cdot \nabla T) \tag{1}$$

under constant pressure, the enthalpy E is defined as

$$\left(\frac{dE}{dt}\right)_p = C_p(T) \tag{2}$$

where the ρ, k, C_p are the density, the thermal conductivity, and the specific heat, respectively.

According to the assumption that the phase changes occur over a temperature range: $\Delta T = T_2 - T_1$, and the specific heats for each phase are constant, we have

$$T = \begin{cases} T_1 + E/C_s & \mathrm{E} \le 0 \\ T_1 + \Delta T \cdot E/(H + C_m \cdot \Delta T) & 0 < \mathrm{E} < \mathrm{H} + \mathrm{Cm} \cdot \Delta \mathrm{T} \\ T_1 + E/C_l - [H + (C_m - C_l) \cdot \Delta T]/C_l & \mathrm{E} \ge \mathrm{H} + \mathrm{Cm} \cdot \Delta \mathrm{T} \end{cases} \tag{3}$$

where C_s, C_l, C_m are the specific heats of the solid phase, liquid phase and the phase-change region, respectively. Here H is the latent heat released within the phase-change process.

According to the foregoing assumptions and definite condition, we have

$$\begin{cases} T = T_0 & \text{for} \quad \mathrm{t} = 0, \quad 0 < \mathrm{x} < \mathrm{L} \text{ (initial condition)} \\ T = T_W & \text{for} \quad \mathrm{t} \ge 0, \quad \mathrm{x} = \mathrm{L} \quad \text{(boundary condition, at the metallic wall surface)} \\ -k_1 \cdot \frac{\partial T}{\partial x} = h_g \cdot (T - T_g) & \text{for} \quad t \ge 0, \quad x = 0 \quad \text{(bounary condition, at the gas/melt interface}^{33,34}\text{)} \end{cases} \tag{4}$$

where h_g, T_g are the heat transfer coefficient and the temperature of gas, respectively. Then the Kirchhoff temperature[26] is introduced:

$$T_{kir} = \Gamma(E) \cdot E + S(E) \tag{5}$$

Thus, the enthalpy transformation equation becomes,

$$\rho \cdot \frac{\partial E}{\partial t} = \frac{\partial^2(\Gamma \cdot E)}{\partial x^2} + \frac{\partial^2 S}{\partial x^2} \tag{6}$$

Now the enthalpy transformation from the normal linear energy equation to the nonlinear equation ends up with a single variable E. Then, the finite-difference scheme is used for the discretization and calculation procedures.

To discretize eq. (6) and the related definite conditions, the Patankar's methodology[35] of control volume/finite difference approach was used. For the numerical calculation procedures, the iterative formulations for eq. (6) can be written as:

$$E_i^{j+1} = \xi \cdot \left[\Gamma_{i-1}^j \cdot E_{i-1}^j + S_{i+1}^j + \Gamma_{i+1}^j \cdot E_{i+1}^j + S_{i-1}^j - 2 \cdot \frac{(2\Gamma_i^j - 1)}{2} \cdot E_i^j - 2 \cdot S_i^j) \right] \tag{7}$$

then the corresponding discretization forms of the initial and boundary conditions are given as:

$$\begin{cases} E_1^j = (T_W - T_1) \cdot C_s; \quad \mathrm{j} = 1,2,3,..., \\ E_i^0 = (T_0 - T_1) \cdot C_l + H + (C_m - C_l) \cdot \Delta T; \quad \mathrm{i} = 1,2,3,...,\mathrm{n} \\ E_n^j = E_{n-1}^j - \frac{\Delta x \cdot h_g}{k_l \cdot \left[E_{n-1}^j + C_l \cdot (T_1 - T_g) - H\right]}; \quad \mathrm{j} = 1,2,3,..., \end{cases} \tag{8}$$

with $\xi = \Delta t/(\rho \Delta x^2)$, where Δt, Δx, and ρ are the time increment, the space step along the x-axis, and the density of HDPE. The earlier discretization leads to stable and convergent numerical solutions when the following criterion is satisfied:

$$0 \le \frac{k_s \cdot \Delta t}{\rho \cdot C_s \cdot (\Delta x)^2} \le \frac{1}{2} \tag{9}$$

Figure 6 shows the discrete mesh and the liquid-solid moving interface in the numerical calculations. Here the time increment Δt is of the order of 0.01 (s), e.g., $\Delta t = 0.05$ s. When the E field is determined from the earlier iterative procedures (with detailed iterations omitted), the temperature field can be calculated from eq. (3).

In the earlier formulation with regard to the phase-change zone, for simplicity, a linear change

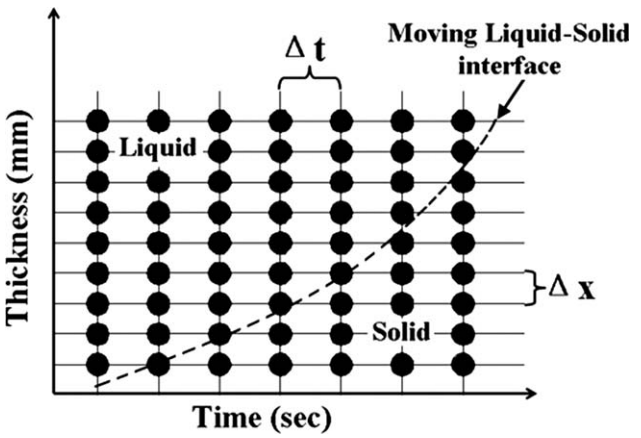

Figure 6 Schematic of the discretized meshes and the liquid/solid interface in the numerical domains.

was applied, thus, we have C_m, k_m as: $C_m = (C_s + C_l)/2$, $k_m = (k_s + k_l)/2$.

RESULTS AND DISCUSSION

Simulations of the temperature profiles

To simulate the solidification behaviors of HDPE using the mathematical modeling, comparisons were made accordingly. For the purpose of simplification, normalized distance was introduced and defined by $\chi = x/b$, where b is the part thickness, i.e., the reference length in this case. Figure 7 shows the simulated temperature profiles under the experimental conditions: $T_0 = 190°C$, $T_W = 15°C$, during 10–70 s, which are obtained via the aforementioned discretization and calculation procedures. The region between the two horizontal reference lines of $T = 110°C$ and $T = 120°C$ represents the phase-change zone, which separates the liquid phase away from the solid phase. Three main stages of the cooling process are shown in Figure 7. In the initial stage, e.g., $t \leq 40$ s, the cooling system consists of the liquid phase, solid phase, and phase-change region, and the thermal conductance can readily transfer away the released heat associated with the solidification process as well as the sensible heat from the liquid phase, primarily owing to the thin solid layer of polymer near the metallic wall. When 40 s $\leq$ t $\leq$ 60 s, the cooling profiles of 40 s, 50 s, 60 s are quite similar, especially at the end of the curves, and the separation distance is relatively small as compared with that of 10–40 s or 60–70 s, which is mainly because the temperature of the liquid phase reaches the phase change temperature (range), and the latent heat H is released to compensate the thermal dissipation. When $t > 60$ s, there merely exists the solid phase in the cooling system, in that the phase-change process has come to an end, and no thermal compensation theoretically existed. As a consequence, the profile becomes flat.

In addition, it is found that the temperature of the gas/melt interface is not the highest, which is especially true during an initial stage of cooling (e.g., $t \leq 20$ s). As the thermal diffusivities of the polymer and gas are extremely low, the heat released because of crystallization near the skin cannot be transferred away timely from the gas/melt interface. As a result, the temperature increased at some location between the container wall and the gas over a period of time. According to our previous work,[10–14] both shear and temperature fields in GAIM play a significant part in the formation of the crystalline morphologies, such as shish-kebab,[13] banded spherulite,[14] and orientation of lamellae.[36] It will be of significance to investigate the relationship between the temperature and shear rate distributions in our future work.

Experimental verifications

For better comprehension, the normalized temperature and the normalized time introduced by and defined as follows:[37]

$$\theta = \frac{(T - T_w)}{(T_0 - T_w)} = \text{Dimensionless temperature} \quad (10)$$

$$\tau = \frac{\alpha \cdot t}{b^2} = \text{Dimensionless time} \quad (11)$$

where b is the reference length (the thickness in this case), and α the thermal diffusivity, which is defined by $\alpha = k/(\rho \cdot C_p)$. τ is a measure of the rate of heat conduction in comparison with the rate of heat storage within a given volume element.[37]

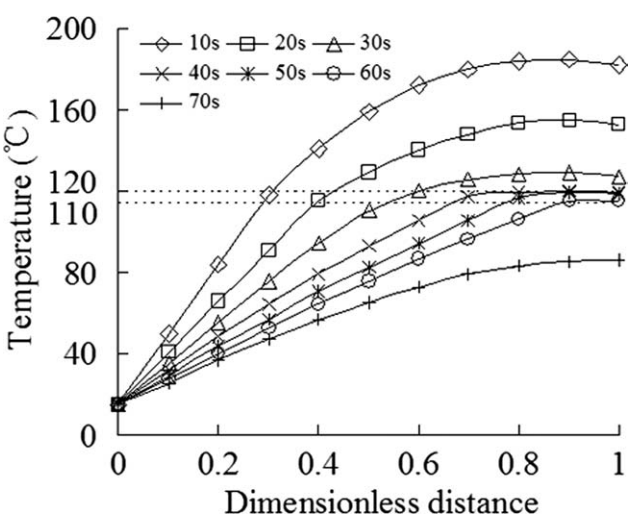

Figure 7 Simulated temperature distribution under the cooling conditions: $T_0 = 190°C$, $T_W = 15°C$.

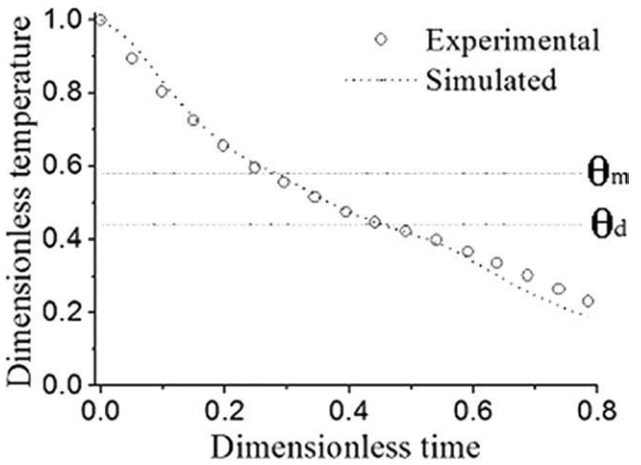

Figure 8 Comparison between the simulated and experimental cooling profiles.

Figure 8 shows the comparison between the simulated and experimental temperature distributions, with the horizontal lines representing the reference temperature of phase change θ_m and demolding temperature θ_d in their dimensionless form, respectively. Based on Figure 8, when $\tau \leq 0.4$, a good agreement was reached between the experimental and simulated data; the mainly discrepancies exist when $0.4 \leq \tau \leq 0.8$, and in this range, the experimental temperature is higher than the simulated temperature. This could be caused by the crystallinity of the polyethylene, owing to the polydispersity and hierarchical structures of the polymers, the polymers cannot achieve the crystallization process like the small molecules, under the experimental conditions crystallization will continue even after the polymers completely solidify, which is different from the theoretical model. As a result, the real heats released will be lower than the theoretical values. Besides, the flow rate of the circulating water in the present simple experiment may not be as the high as that in the mold, the heat released cannot be transfer so readily as in the real cooling stage of the GAIM process. Hence, the experimental temperatures are a bit higher than the simulated results.

The experimental and theoretical cooling rates, in accordance with Brucato et al.,[38] are calculated and listed in Table I. The simulated data agree well with the experimental results, and the experimental instantaneous cooling rates are in agreement with our previous studies of GAIM process.[30] In our previous work, cooling rates in different location have been discussed in both GAIM and CIM processes. It was found that when $\chi = 0.31$, the phase-change plateau was only observed in CIM process, rather than in GAIM. In the present article, the phase-change plateau does not exist, either, and this to some extent proved the cooling rates can affect the shape of the cooling curves.

TABLE I
Cooling Rates Obtained from the Experiment and Simulations

Cooling rates	Experimental (°C/s)	Theoretical (°C/s)
Average cooling rate (τ = 0–0.3)	2.690	2.483
Instantaneous cooling rate (τ = 0.3)	1.449	1.493

The dimensionless cooling time obtained from experiment is 0.45 (t = 48 s), and the theoretical cooling time is 0.44 (t = 45 s). On the whole, both the experimental and the theoretical results agree well. The experimental cooling time is a little larger than the theoretical one, which may be caused by thermal diffusivity of the metallic container wall. Because of the thermal diffusivity of the metallic container wall is smaller than the ideal mold wall, the heat in the metallic container wall cannot be transferred away as readily as that in the real mold wall. Besides, the thickness of the melt in the metallic container is not always a constant in the experiment condition; with the polymer shrinkage effects, the thermal parameters of the material would be different from those under the theoretical conditions. Thus, the experimental data are slightly different from the theoretical ones. However, the simulated results are reasonable, allowing for the aforementioned discrepancies.

In short, through the comparison between the experimental results and the theoretical predictions, the results are acceptable, which indicates that this simple experimental method coupled with numerical simulation approach can be applied to predict the temperature profile and cooling time of the GAIM process. Anyway, it should be noted that the crystallization kinetics should also be taken into account quantitatively so as to further improve the precision of numerical prediction. In addition, improvement on the experimental equipment should be considered in our further work.

CONCLUSIONS

In the present article, a simple approach was applied to forecast the cooling time of high-density polyethylene during the GAIM process. A simple and *in situ* experimental method coupled with numerical simulation schemes was applied to predict the cooling time of the GAIM process. Experiments were carried out in a specially-designed *in situ* instrument, which simulated the cooling stage of the GAIM process, and good agreement was observed from the comparison between the experimental and simulated results, under some reasonable assumptions and definite

conditions. However, some discrepancies were still observed, mainly because of the crystallization kinetics as well as the polymer shrinkage effects, allowing for the uncertainty of the thermal parameters and the assumptions introduced. Moreover, this simple method will probably be used for further study of the crystailline morphology of the GAIM parts and optimal designs of the GAIM process for industrial applications.

NOMENCLATURE

C_p	Heat capacity, $J \cdot kg^{-1} \cdot {}^\circ C^{-1}$
E	Enthalpy, $J \cdot kg^{-1}$
k	Thermal conductivity, $W \cdot m^{-1} \cdot {}^\circ C^{-1}$
h	Heat transfer coefficient, $W/m^2 \cdot {}^\circ C$
H	Latent heat, $J \cdot kg^{-1}$
S	Coefficient in eq. (5)
Γ	Coefficient in eq. (5)
T	Temperature, °C
T_0	Initial temperature, °C
T_1	Lower boundary temperature of the phase-change zone, °C
T_2	Upper boundary temperature of the phase-change zone, °C
T_m	Reference temperature, defined by $T_m = (T_1+T_2)/2$, °C
T_g	Gas temperature, °C
T_{kir}	Kirchhoff temperature, W/m
T_w	Water temperature, °C
t	Time, s
Δt	Time increment, s
x	Distance along x-axis direction, m
Δx	Space step along x-axis direction, m
α	Thermal diffusivity, defined by $\alpha = k/(\rho \cdot C_p)$
ρ	Material density, $kg \cdot m^{-3}$
τ	Fourier number (Fo) or dimensionless time, defined by eq. (11)
ξ	Coefficient defined by eq. (7)
χ	Dimensionless distance along the x-axis
θ	Dimensionless temperature, defined by eq. (10)

Subscripts

w	Water
g	Gas
s	Solid phase
l	Liquid phase
m	Phase-change region

The authors thank Jian-Ming Feng (Sichuan University) for experimental assistance and helpful discussions. In particular, the authors are very grateful to the referees for their insightful comments and suggestions for improvements of this contribution.

References

1. Turng, L. S. Adv Polym Technol 1995, 14, 1.
2. Li, C. T. Polym Eng Sci 2004, 44, 992.
3. Turng, L. S. Adv Polym Technol 1997, 16, 159.
4. Zhou, H. M.; Li, D. Q. App Math Modell 2003, 27, 849.
5. Parvez, M. A.; Ong, N. S.; Lam, Y. C. J. Mater Process 2002, 121, 27.
6. Chen, S. C.; Hsu, K. S.; Hung, J. S. Ind Eng Chem Res 1995, 34, 416.
7. Ong, N. S.; Lee, H. L.; Parvez, M. A. Adv Polym Tech 2001, 20, 270.
8. Chen, L.; Li, J. H.; Zhou, H. M.; Lib, D. Q.; He, Z. C.; Tang, Q. J. Mater Process Technol 2008, 208, 90.
9. Polynkin, A.; Pittman, J. F. T.; Sienz, J. Polym Eng Sci 2005, 45, 1049.
10. Zheng, G. Q. A.; Huang, L.; Yang, W.; Yang, B.; Yang, M. B.; Li, Q.; Shen, C. Y. Polymer 2007, 48, 5486.
11. Zheng, G. Q.; Yang, W.; Huang, L.; Yang, M. B.; Li, W.; Liu, C. T.; Shen, C. Y. Mater Lett 2007, 61, 3436.
12. Zheng, G. Q.; Yang, W.; Huang, L.; Li, Z. M.; Yang, M. B.; Yin, B.; Li, Q.; Liu, C. T.; Shen, C. Y. J Mater Sci 2007, 42, 7275.
13. Huang, L.; Yang, W.; Yang, B.; Yang, M. B.; Zheng, G. Q.; An, H. N. Polymer 2008, 49, 4051.
14. Zheng, G. Q.; Yang, W.; Yang, M. B.; Chen, J. B.; Li, Q.; Shen, C. Y. Polym Eng Sci 2008, 48, 976.
15. Katti, S. S.; Schultz, J. M. Polym Eng Sci 1982, 22, 1001.
16. Crank, J. Free and Moving Boundary Problems; Clarendon Press: Oxford, 1984.
17. Bondarev, V. A. Int J Heat Mass Transfer 1997, 40, 3487.
18. Gorla, R. S. R.; Canter, M. S.; Pallone, P. J. Heat Mass Transfer 1998, 33, 439.
19. Westerberg, K. W.; Wiklof, C.; Finlayson, B. A. Numer Heat Transfer Part B: Fund 1994, 25, 119.
20. Hsieh, C. K. Trans ASME 1995, 117, 1076.
21. Aziz, A.; Jaleel, A.; Haneef, M. Chem Eng J Biochem Eng J 1980, 19, 171.
22. Parang, M.; Crocker, D. S.; Haynes, B. D. Int J Heat Fluid Flow 1999, 11, 142.
23. Lin, P.; Jaluria, Y. Polym Eng Sci 1997, 37, 1247.
24. Ferreira, I. L.; Spinelli, J. E.; Pires, J. C.; Garcia, A. Mater Sci Eng Part A: Struct 2005, 408, 317.
25. Jana, S.; Ray, S.; Durst, F. Appl Math Modell 2007, 31, 93.
26. Cao, Y.; Faghri, A. Int J Heat Mass Transfer 1989, 32, 1289.
27. Tao, S. P.; Fu, X. R.; Yang, M. B.; Yu, R. Z. Acta Polym Sinica 2005, 1, 8.
28. Bai, Y.; Yin, B.; Fu, X. R.; Yang, M. B. J Appl Polym Sci 2006, 102, 2249.
29. Yang, B.; Fu, X. R.; Yang, W.; Huang, L.; Yang, M. B.; Feng, J. M. Polym Eng Sci 2008, 48, 1707.
30. Yang, B.; Fu, X. R.; Yang, W.; Liang, S. P.; Hu, S.; Yang, M. B. Polym Eng Sci 2009, 49, 1234.
31. Yang, B.; Fu, X. R.; Yang, W.; Liang, S. P.; Sun, N.; Hu, S.; Yang, M. B. Macromol Mater Eng 2009, 294, 336.
32. Kays, W. D.; Crawford, M. E. Convective Heat and Mass Transfer, 2nd ed; McGraw-Hill: New York, 1980.
33. Chang, Y. P.; Hu, S. Y.; Chen, S. C. Int Commun Heat Mass Transfer 1998, 25, 989.
34. Chen, S. C.; Hu, S. Y.; Chao, S. M.; Chien, R. D. Polym Eng Sci 2000, 40, 595.
35. Patankar, S. V. Numerical Heat Transfer and Fluid Flow; McGraw-Hill: New York, 1980.
36. Hu, S.; Yang, W.; Liang, S. P.; Yang, B.; Yang, M. B. J Macromol Sci Phys 2009, 48, 1084.
37. Özisik, M. N. Heat Conduction; Wiley: New York, 1980.
38. Brucato, V.; Piccarolo, S.; La Carrubbab, V. Chem Eng Sci 2002, 57, 4129.